Article

Inhibition of Cholinesterases by Benzothiazolone Derivatives

Mehmet Abdullah Alagöz [1,†], Seong-Min Kim [2,†], Jong Min Oh [2], Gülnur Arslan [3], Zeynep Özdemir [1], Suat Sari [4], Azime Berna Özçelik [5], Tijen Önkol [5], Daniela Trisciuzzi [6], Orazio Nicolotti [6], Hoon Kim [2,*] and Bijo Mathew [7,*]

1   Department of Pharmaceutical Chemistry, Faculty of Pharmacy, Inonu University, Malatya 44280, Turkey
2   Department of Pharmacy, and Research Institute of Life Pharmaceutical Sciences, Sunchon National University, Suncheon 57922, Korea
3   Department of Pharmaceutical Chemistry, Faculty of Pharmacy, Suleyman Demirel University, Isparta 32000, Turkey
4   Department of Pharmaceutical Chemistry, Faculty of Pharmacy, Hacettepe University, Ankara 06230, Turkey
5   Department of Pharmaceutical Chemistry, Faculty of Pharmacy, Gazi University, Ankara 06330, Turkey
6   Dipartimento di Farmacia—Scienze del Farmaco, Univer sità degli Studi di Bari "Aldo Moro", Via E. Orabona, 4, I-70125 Bari, Italy
7   Department of Pharmaceutical Chemistry, Amrita School of Pharmacy, Amrita Vishwa Vidyapeetham, AIMS Health Sciences Campus, Kochi 682041, India
*   Correspondence: hoon@sunchon.ac.kr (H.K.); bijovilaventgu@gmail.com or bijomathew@aims.amrita.edu (B.M.)
†   These authors contributed equally to this work.

Abstract: Thirteen benzothiazolone derivatives (**M1**–**M13**) were synthesized and evaluated for their inhibitory activity against cholinesterases (ChEs) and monoamine oxidases (MAOs). All the compounds inhibited ChEs more effectively than MAOs. In addition, most of the compounds showed higher inhibitory activities against butyrylcholinesterase (BChE) than acetylcholinesterase (AChE). Compound **M13** most potently inhibited BChE with an IC_{50} value of 1.21 μM, followed by **M2** (IC_{50} = 1.38 μM). Compound **M2** had a higher selectivity index (SI) value for BChE over AChE (28.99) than **M13** (4.16). The 6-methoxy indole group of **M13** was expected to have a greater effect on BChE inhibitory activity than the other groups. Kinetics and reversibility tests showed that **M13** was a reversible noncompetitive BChE inhibitor with a K_i value of 1.14 ± 0.21 μM. In a docking simulation, **M13** is predicted to form a hydrogen bond with the backbone carbonyl group of Ser287 of BChE through its methoxy indole moiety and π−π interactions between its benzothiazolone group and the side chain of Trp82 with the five-membered pyrrole ring and with the six-membered benzene ring. From these results, it is suggested that **M13** is a BChE inhibitor and a potential candidate agent for the treatment of Alzheimer's disease.

Keywords: benzothiazolone; cholinesterase inhibitor; kinetics; docking analysis

1. Introduction

As for the general consideration, Alzheimer's disease (AD) is associated with neuron loss in the brain; however, the pathophysiological events leading to neuron loss are yet to be entirely understood. According to the cholinergic hypothesis, the reduction of acetylcholine, a crucial neurotransmitter, is assumed to be the cause of AD [1,2]. In AD patients, cholinergic neurons in the basal forebrain degenerate, and levels of cholinergic receptors and choline acetyltransferase in the cerebral cortex are found to be significantly decreased [3]. Clinical trials have shown that medications focused on raising acetylcholine levels offer symptomatic alleviation, with the fact that many previous treatment methods were founded on this concept [4,5]. According to recent research on the cholinergic hypothesis, amyloid fibrillation, one of the pathological signs of AD, may be influenced by the use of cholinesterase inhibitors [6–8].

Some cholinesterase (ChE) inhibitors, such as rivastigmine, tacrine, galantamine, donepezil, and huperzine A, have been shown to slow the progression of AD. Tacrine (Cognex[®]), the first drug among these compounds approved by the FDA in the USA for the treatment of AD, is based on the cholinergic hypothesis of AD as an acetylcholinesterase (AChE) inhibitor and was put into clinical use. However, due to its hepatotoxicity, tacrine has been limited in clinical use. By contrast, three other AChE inhibitors, rivastigmine, donepezil, and galantamine, were approved as anti-AD drugs and used clinically. These drugs also show effects other than AChE inhibition. Rivastigmine can block butyryl-cholinesterase (BChE), while galantamine can modulate nicotinic acetylcholine receptors [8,9]. Donepezil is a moderate inhibitor of β-amyloid (Aβ) synthesis and the β-secretase (BACE1) responsible for Aβ synthesis, and it can also interact with sigma-1 receptors, which are known for their anti-amnesic activities [10].

Structural features and key binding sites of residues of AChE and BChE active sites have been clarified by crystallographic studies with molecules known to be AChE and BChE inhibitors, such as tacrine, donepezil, and galantamine [11–17]. Studies have determined that there is a catalytic active site (CAS), peripheral anionic site (PAS), anionic subsite (AS), oxyanion hole, and acyl binding pocket in the active site of the enzyme. It has been reported that the interactions with residues in the CAS, PAS, and AS cause significant changes in the activity of the enzyme. Contrary to tacrine, donepezil and galantamine interact with the cationic active site (CAS), the acyl-binding pocket, and the PAS residues that surround the rim at the entry to the active gorge [12,17–20]. The acetylcholine bond breaking is catalyzed by the catalytic triad of three amino acids, S203, E334, and H447, which are located at the bottom of this gorge [21]. The ideal scenario would be for an agent to interact with these active regions of the enzyme by inhibiting ChE (Figure 1a). Despite a 65% sequence similarity between BChE and AChE, there are notable differences that are crucial for the enzyme's selectivity, for example, the larger acyl-binding pocket in BChE [22].

It has been reported that the benzoxazolone ring has many important activities, such as anticancer, antimicrobial, antiviral, antioxidant, analgesic, anti-inflammatory, and ChE inhibitory activities. The benzoxazolone ring was defined as a "privileged skeleton" because of its high chemical reactivity and wide variety of biological activities [23–26]. In addition, various tertiary amine moieties have been reported as a pharmacophore group in ChE inhibition, including the importance of designing compounds with a benzoxazolone structure containing the tertiary amine moieties with a ChE inhibition effect [27,28].

It has been reported in the literature that various compounds carrying the benzothiazolone skeleton have ChE inhibitory effects. Erdogan et al. investigated the ChE inhibitory activity of some benzothiazol-2-one derivatives and reported the most effective compound (Figure 1b) with an IC$_{50}$ value of 0.34 μM against AChE [23]. The synthesized compounds (**M1-13**) were derived from the 3rd position of the benzothiazolone core, and the most active compound (Figure 1b) was derived from the 6th position of the core. When compound **M13** and the most active compound are evaluated, both compounds have a benzothiazol-2-one core in the peripheral anionic region. **M13** and the most effective compound (Figure 1b) have a 6-methoxyindole group and phenyl ring at the choline-binding site, respectively, as well as an acetohydrazide structure and a piperazine ring at the positive charge center.

In addition, various compounds have been designed and synthesized as ChE inhibitors using Schiff bases as linkers. The compounds were observed to be potentially useful for ChE inhibition and possible treatment for AD (Figure 1c,d) [29,30].

In light of this information, in the present study, we aimed to synthesize and characterize benzothiazolone derivatives, i.e., the M series, and determine their ChE inhibitory activity according to the hypothesis as shown below (Figure 2).
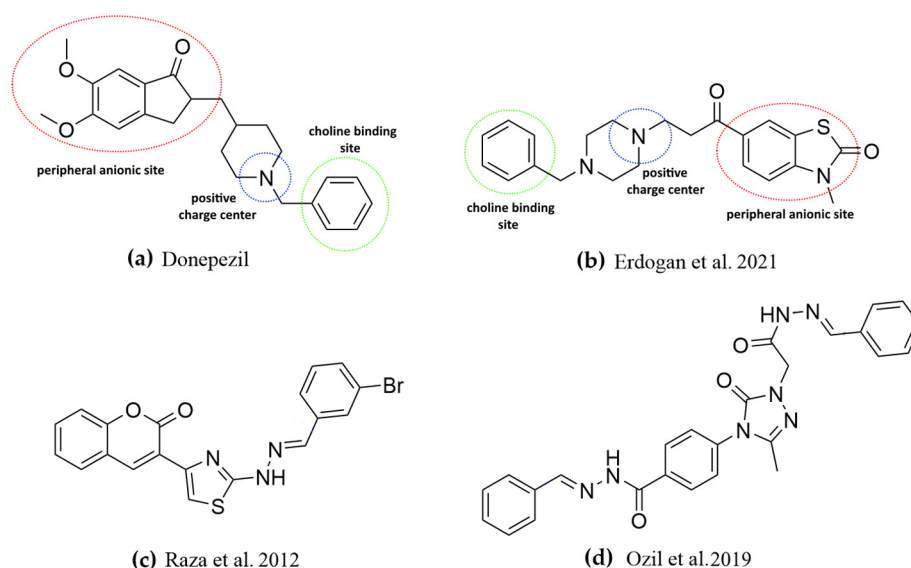
Figure 1. Structural hypothesis for ChE inhibitors illustrated on donepezil (**a**) and a bezothiazolone derivative (**b**) and ChE inhibitor Schiff base derivatives (**c**,**d**) [23,29,30].
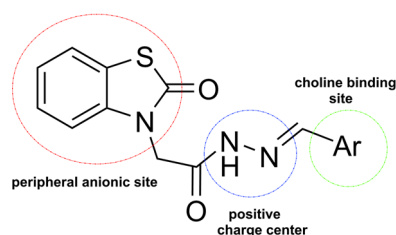

Figure 2. Structural hypothesis for the M series.

2. Materials and Methods

2.1. Experimental Procedure for Synthesis

General procedure of synthesis:

Benzo[d]thiazol-2(3H)-one (**1**): A mixture of 2-aminothiophenol [1 eq] and urea [2 eq] was taken into a flask and irradiated in a microwave oven at 140 °C and 500 W for 15 min without a solvent. The reaction was cooled and poured into ice water, and the resulting solid was filtered off. The solid obtained was added to a 10% NaOH solution and filtered, and the filtrate was acidified with concentrated hydrochloric acid. The precipitate was filtered off, dried, and crystallized from water. The product was obtained with an 87% yield. The reaction was monitored with TLC and LC-MS [31].

Ethyl 2-(2-oxobenzo[d]thiazol-3(2H)-yl)acetate (**2**): Benzo[d]thiazol-2(3H)-one 1 eq], ethyl bromoacetate [1.2 eq], K_2CO_3 [2 eq], and acetone were mixed at 400 W at 58 °C for 20 min. The reaction was cooled and taken up in ice water, and the precipitated solid was filtered off, washed with water, and dried. The product was obtained in 91% yield. The reaction was monitored with TLC and LC-MS [32].

2-(2-oxobenzo[d]thiazol-3(2H)-yl)acetohydrazide (**3**): Ethyl 2-(2-oxobenzo[d]thiazol-3(2H)-yl)acetate [1 eq] was dissolved in ethanol and hydrazine hydrate [10 eq] was added dropwise and refluxed at 70 °C for 3 h. The reaction was cooled, and the solid formed was filtered and dried. The product was obtained with an 82% yield. The reaction was monitored with TLC and LC-MS [33].

2-(2-oxobenzo[d]thiazol-3(2H)-yl)-N′-(substitued)acetohydrazide derivatives (**M1**–**M13**): 2-(2-Oxobenzo[d]thiazol-3(2H)-yl)acetohydrazide [1 eq] and its aldehyde derivatives [1.2 eq] were mixed in 5 mL of acetic acid at 400 W for 10 min at 85 °C. The reaction was cooled, taken up in ice water, and filtered, and the solid in ethanol:water [8:2] was

crystallized, and the crystals were filtered and adjusted. The products were obtained with a 55–75% yield. The reaction was monitored with TLC and LC-MS.

General information about materials and methods for the chemistry is described in the Supplementary information (Method S).

2.2. Inhibition Studies of ChE and MAO

Using 0.5 mM of acetylthiocholine (ATCI) and butyrylthiocholine iodide (BTCI) as substrates, respectively, the inhibitory activity of AChE and BChE were evaluated for 15 min at 412 nm. For the colour development, 0.5 mM of 5,5-dithiobis (2-nitrobenzoic acid) (DTNB) was also added [34]. AChE from Electrophorus electricus and BChE from horse serum were used for the ChEs. Before adding BTCI and DTNB, AChE or BChE was mixed with an inhibitor and preincubated for 10 min. Thiocholine, an AChE or BChE reaction product, and DTNB form the yellowish 5-thio-2-nitrobenzoic acid. According to a prior description, the activities of MAO-A and MAO-B were monitored continuously for 45 min at 316 nm using 0.06 mM of kynuramine and at 250 nm using 0.3 mM of benzylamine, respectively, as described previously [35].

2.3. Enzyme Inhibition and Kinetic Studies

After inhibitory activities of the compounds for ChEs or MAOs were evaluated at a concentration of 10 μM, an IC_{50} value of each compound showing residual activity of <50% was determined. The IC_{50} value was calculated by measuring the residual activity at different concentrations of the compound and by using GraphPad Prism software 5 [36,37]. The selectivity index (SI) value of BChE was calculated by (IC_{50} of AChE)/(IC_{50} of BChE) [38]. Enzyme kinetic parameters, inhibitor type, and K_i value of compound **M13** were determined by measuring enzyme activity at five different substrate concentrations and at three different inhibitor concentrations (0.5–2 times of IC_{50}) [39,40]. The inhibition type and K_i value were determined by the Lineweaver–Burk plots and their secondary plots, respectively.

2.4. Reversibility Analysis of M13

The reversibility of BChE inhibition by **M13** was evaluated using dialysis after preincubation of BChE and **M13** for 10 min at ~2.0 × IC_{50} (i.e., 2.42 μM), as previously described [41]. For the reference compound, donepezil (a reference reversible BChE inhibitor) was preincubated at ~2.0 × IC_{50} (0.36 μM). The reversibility pattern was determined by comparing the activities of dialyzed (A_D) and undialyzed (A_U) samples.

2.5. Docking Studies

First of all, the three-dimensional X-ray structures of hAChE (PDB ID: 4EY7 [17]) and hBChE (PDB ID: 6RUA [42]) were retrieved from the Protein Data Bank (PDB). The target structures were refined using Protein Preparation Wizard (Schrödinger Suite 2021–4) [43] in order to correct the bond order and to add hydrogen atoms and possible missing amino acidic side chains and loops.
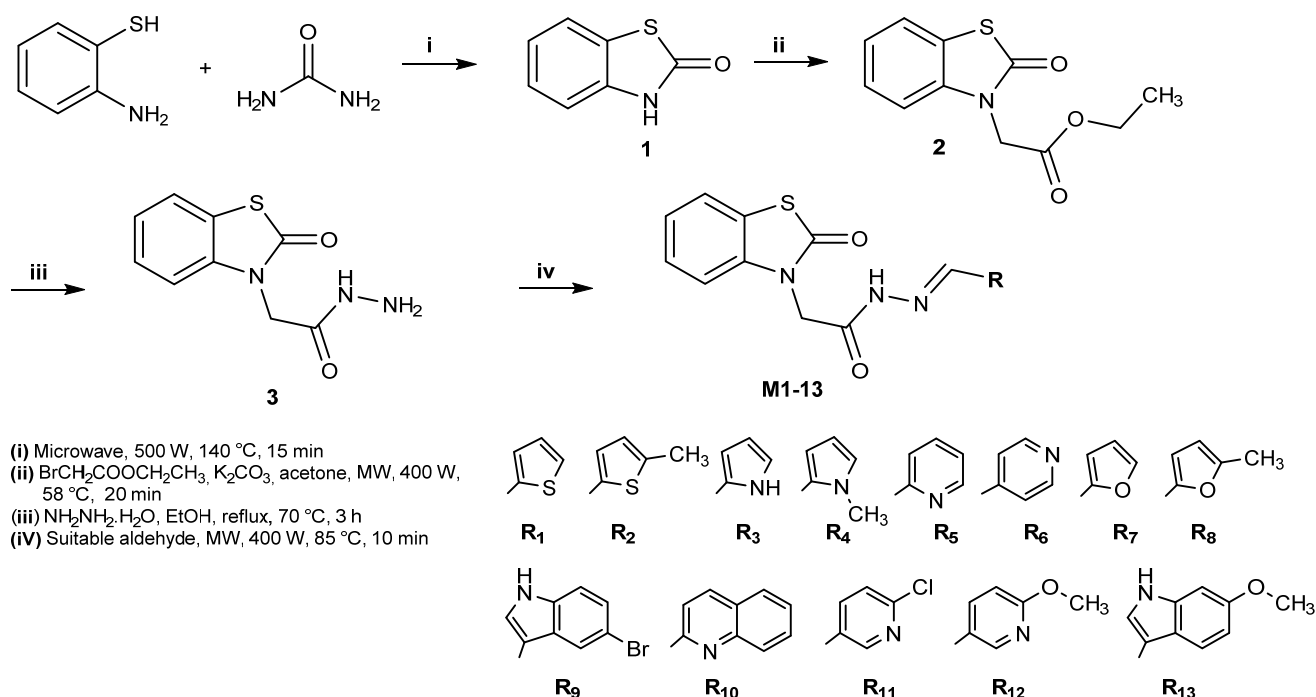
The 3D conformation of the compound **M13** was processed by LigPrep (Schrödinger Suite 2021–4) [44] in order to properly generate all the possible tautomers and ionization states at a physiological pH value of 7.4. For the co-crystallized cognate ligands (donepezil and KJT for 4EY7 and 6RUA, respectively), cubic grids for hAChE and hBChE were generated. The edges of the inner and outer boxes were 10 × 10 × 10 Å and 28 × 28 × 28 Å, and 10 × 10 × 10 Å and 24 × 24 × 24 Å, respectively.

Docking simulations were, thus, performed using Grid-based Ligand Docking with Energetics (GLIDE) v.9.1 [45,46], which is a part of the Schrodinger Suite (Schrödinger Suite 2021–4). All the default advanced settings for standard precision (SP) were used, and the Force Field OPLS_2005 was employed. The reliability of an SP simulation protocol was previously challenged by computing the Root Mean Square Deviation (RMSD) values.

3. Results and Discussion

3.1. Chemistry

The title compounds (**M1–M13**) were synthesized in accordance with the literature, as shown in Scheme 1.

(i) Microwave, 500 W, 140 °C, 15 min
(ii) BrCH$_2$COOCH$_2$CH$_3$, K$_2$CO$_3$, acetone, MW, 400 W,
   58 °C, 20 min
(iii) NH$_2$NH$_2$.H$_2$O, EtOH, reflux, 70 °C, 3 h
(iv) Suitable aldehyde, MW, 400 W, 85 °C, 10 min

Scheme 1. Synthesis of the compounds **M1-13**.

Synthesis-starting material benzo[d]thiazol-2(3H)-one **(1)** was synthesized using 2-aminothiophenol and urea with an 87% yield according to the microwave irradiation method. As a result of the reaction of the resulting compound **(1)** with ethyl bromoacetate, ethyl 2-(2-oxobenzo[d]thiazol-3(2H)-yl)acetate **(2)** was obtained in high yield (91%) by the microwave irradiation method. Compound 2-(2-oxobenzo[d]thiazol-3(2H)-yl)acetohydrazide **(3)** was synthesized by the reaction of compound **2** with hydrazide hydrate in ethanol, and the reaction was completed in 3 h at 70 °C. In the third step **(iii)**, without microwave irradiation, the reaction time was considerably prolonged, and the yield was reduced. The resulting compounds, the Schiff bases (**M1-13**), were obtained by the reaction of compound **3** with substituted and unsubstituted benzaldehyde derivatives. The resulting compounds (**M1–13**) were synthesized in a 55–93% yield (Table 1). The spectral characterization of the compounds (**M1–M13**) is provided in the supplementary information (Figure S).

3.2. Inhibition Studies of ChE and MAO

Thirteen benzothiazolone derivatives were synthesized and tested for ChEs' and MAOs' inhibitory activities. All derivatives showed more effective inhibitory activity against ChEs than MAOs. Based on the residual activity at 10 μM, three and five compounds showed < 50% for AChE and BChE, respectively (Table 2); however, no compounds showed < 50% for MAO-A and MAO-B, except **M10** for MAO-B (Table S1). Compound **M13** most potently inhibited BChE with an IC$_{50}$ value of 1.21 μM, followed by **M2** (IC$_{50}$ = 1.38 μM) (Table 2). In the case of BChE inhibitory activity, the IC$_{50}$ values of **M13** and **M2** were lower than those of glycyrol (7.22 μM) from the roots of *Glycyrrhiza uralensis* [47] and khellactone coumarin 3′,4′-disenecioylkhellactone (7.20 μM) from *Peucedanum japonicum* Thurnberg [48] and sargachromanol I (13.69 μM) from *Sargassum siliquastrum* 20 [36]. Structurally, **M13** and **M9** have a 6-methoxy indole and 5-bromo indole, respectively, whereas **M4** and **M2** have a

1-methyl pyrrole and 5-methyl thiophene, respectively. It is suggested that the 6-methoxy indole group is expected to have a greater effect on BChE inhibitory activity than the other groups. Compound **M2** had a higher selectivity index (SI) value for BChE (28.99) than **M13** (4.16). The substrate preference of AChE and BChE is different; AChE prefers ACh, while BChE has a relatively wide substrate range with a low preference for ACh. Therefore, SI values are important in inhibitor screening. On the other hand, all derivatives showed weak MAO inhibitory activities, except **M10** for MAO-B (IC$_{50}$ = 2.75 μM) (Table S1). These results show that **M13** is a potent BChE inhibitor.

Table 1. Structures, yields, melting points, and molecular formula of the synthesized compounds.

Compound	R	Yield (%)	M.P. (°C)	Molecular Formula
M1	thiophen-2-yl	91	250-2	$C_{14}H_{11}N_3O_2S_2$
M2	5-methylthiophen-2-yl	93	284-6	$C_{15}H_{13}N_3O_2S_2$
M3	1H-pyrrol-2-yl	70	238-4	$C_{14}H_{12}N_4O_2S$
M4	1-methyl-1H-pyrrol-2-yl	91	264-6	$C_{15}H_{14}N_4O_2S$
M5	pyridin-2-yl	68	228-30	$C_{15}H_{12}N_4O_2S$
M6	pyridin-4-yl	71	162-4	$C_{15}H_{12}N_4O_2S$
M7	furan-2-yl	71	216-7	$C_{14}H_{11}N_3O_3S$
M8	5-methylfuran-2-yl	80	238-40	$C_{15}H_{13}N_3O_3S$
M9	5-bromo-1H-indol-3-yl	67	268-9	$C_{18}H_{13}BrN_4O_2S$
M10	quinolin-2-yl	59	271-2	$C_{19}H_{14}N_4O_2S$
M11	6-chloropyridin-3-yl	75	237-8	$C_{15}H_{11}ClN_4O_2S$
M12	6-methoxypyridin-3-yl	55	226-7	$C_{16}H_{14}N_4O_3S$
M13	6-methoxy-1H-indol-3-yl	62	262-3	$C_{19}H_{16}N_4O_3S$

Table 2. Inhibitions of ChE by the M series [a].

Compound	Residual Activity at 10 μM (%)		IC$_{50}$ (μM)		SI [b]
	AChE	BChE	AChE	BChE	
M1	61.85 ± 6.48	44.45 ± 0.72	>40	11.55 ± 2.22	>3.46
M2	53.33 ± 0.73	18.08 ± 0.80	>40	1.38 ± 0.17	>28.99
M3	70.22 ± 3.00	67.20 ± 3.63	>40	>40	>1.33
M4	43.17 ± 5.68	41.66 ± 0.28	5.52 ± 0.06	4.55 ± 0.25	1.21
M5	73.61 ± 0.05	70.43 ± 5.13	>40	>40	>1.33
M6	72.15 ± 1.02	80.22 ± 3.82	>40	>40	>1.33
M7	72.89 ± 1.06	76.62 ± 2.89	>40	>40	>1.33
M8	62.34 ± 2.93	62.20 ± 3.12	>40	>40	>1.33

Table 2. *Cont.*

Compound	Residual Activity at 10 μM (%)		IC$_{50}$ (μM)		SI [b]
	AChE	BChE	AChE	BChE	
M9	39.05 ± 1.35	33.42 ± 2.39	8.17 ± 0.28	3.30 ± 0.74	2.48
M10	60.06 ± 1.26	59.30 ± 4.76	32.27 ± 121	17.16 ± 2.92	1.88
M11	68.93 ± 0.84	61.42 ± 1.77	37.25 ± 1.16	11.39 ± 3.09	3.27
M12	60.22 ± 3.22	84.93 ± 0.58	36.22 ± 0.37	>40	<1.21
M13	37.73 ± 1.93	15.82 ± 2.40	5.03 ± 0.93	1.21 ± 0.05	4.16
Donepezil			0.010 ± 0.002	0.180 ± 0.004	

[a] Results are the means ± standard errors of duplicate or triplicate experiments. [b] Selectivity index (SI) values are expressed for BChE over AChE.

3.3. Kinetic Study

The mode of BChE inhibition by **M13** was investigated using Lineweaver–Burk plots. The plots of BChE inhibition by **M13** were linear, and the lines seemed to be intersected at a point on the *X*-axis, showing that **M13** was a noncompetitive inhibitor of BChE (Figure 3a). A secondary plot obtained from the slopes of the Lineweaver–Burk plots against inhibitor concentrations showed that the K_i value of **M13** was 1.14 ± 0.21 μM (Figure 3b). These results suggest that **M13** is a potent noncompetitive inhibitor of BChE. It is similar to the inhibition type of donepezil.
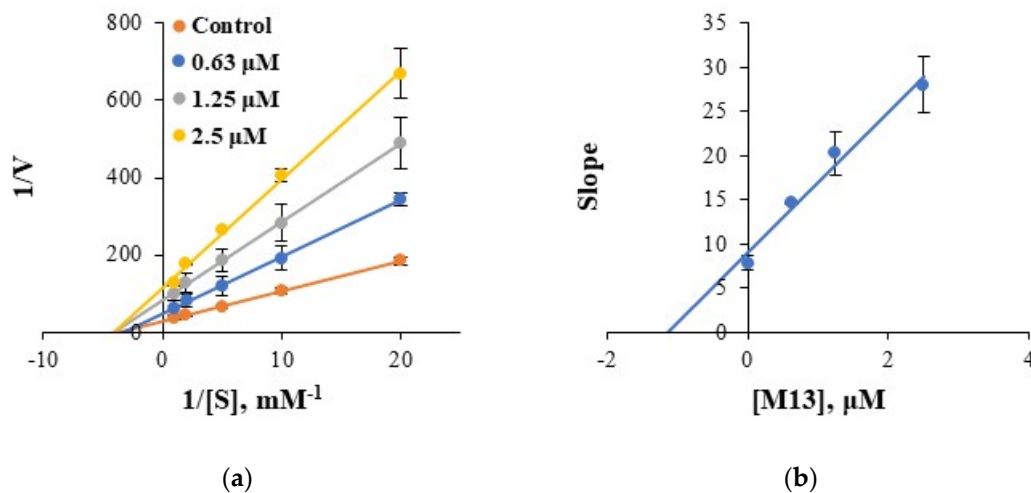

(**a**) (**b**)

Figure 3. Lineweaver–Burk plots for BChE inhibition by **M13** (**a**) and its secondary plot (**b**) of the slopes vs. inhibitor concentrations.

3.4. Reversibility Studies

A reversibility study of BChE inhibition by **M13** was analyzed using the dialysis method. In the experiment, the concentrations used were the following: **M13** at 2.42 μM and donepezil (a reference reversible inhibitor) at 0.36 μM. After dialysis of the preincubated mixture of BChE and **M13**, the relative activities for the undialyzed (A$_U$) and dialyzed (A$_D$) samples were compared to determine the reversibility pattern. As a result, the inhibition of BChE by **M13** was recovered from 30.6% (A$_U$) to 82.2% (A$_D$) (Figure 4). The recovery value for **M13** was similar to that for donepezil (from 29.5% to 88.2%). These results indicate that **M13** is a reversible BChE inhibitor.
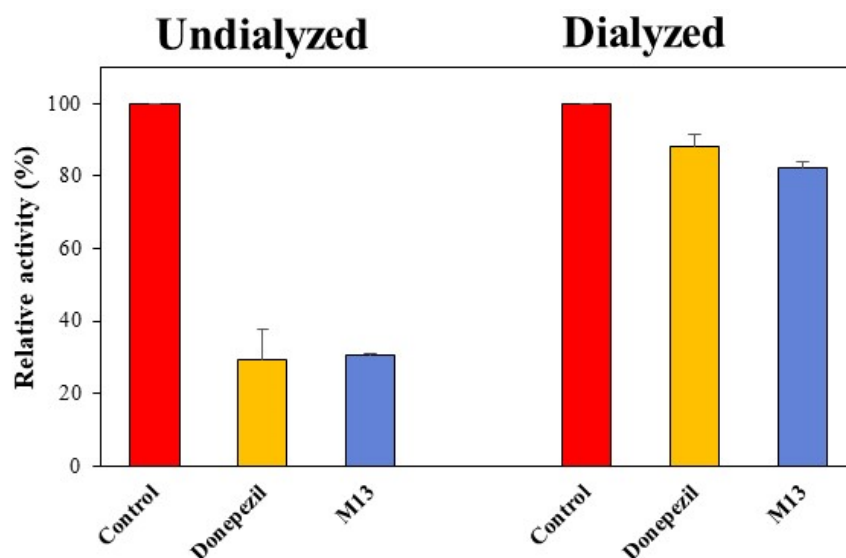
Figure 4. Recovery of BChE inhibition by **M13** using the dialysis method.

3.5. Docking Studies

In order to corroborate the validity of the docking studies, redocking simulations were first performed on the co-crystallized ligands in their binding sites. The cognate ligands moved back to the original positions with RMSD accounting for all the heavy atoms equal to 0.126 Å and 0.686 Å for donepezil and KJT, respectively, whose docking score values were equal to −12.428 and −10.035 kcal/mol, respectively (Figure 5).
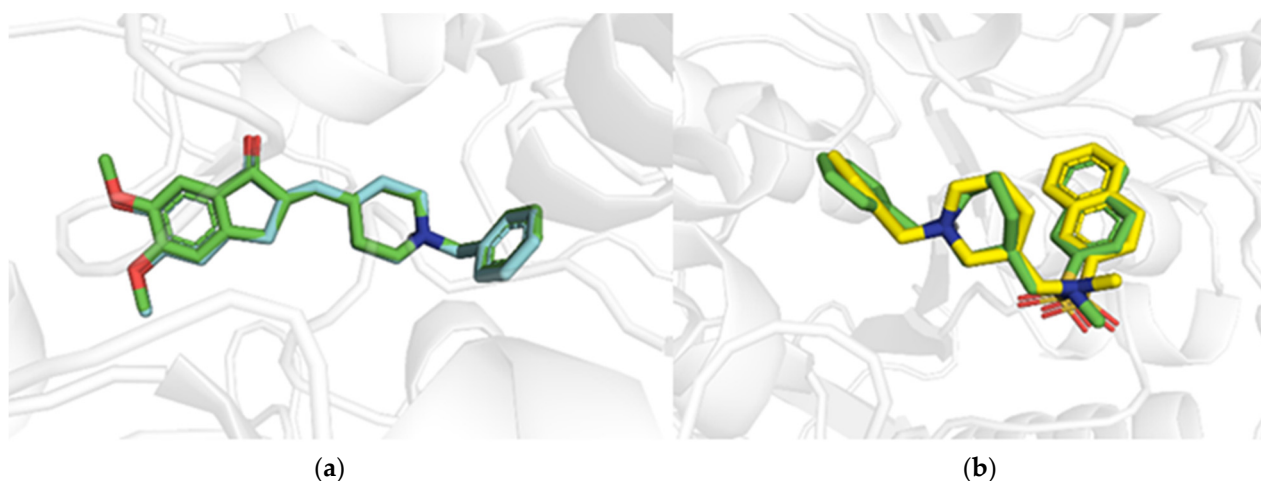

(**a**) (**b**)

Figure 5. Overlaps of the X-ray solved (green sticks) and docking poses for donepezil for hAChE (PDB entry: 4EY7) (**a**) and KJT for hBChE (PDB entry: 6RUA) (**b**), rendering in cyan and yellow sticks, respectively.

The docking simulations were, thus, exploited to investigate the binding modes of the **M13** compound towards the hAChE and hBChE crystal structures. The docking poses of the **M13** compound against both the target proteins, as well as the relevant binding residues, are depicted in Figure 6.

Overall, the molecular docking analyses of **M13** with hAChE and hBChE provide a good rationale for the observed bioactivities. The IC_{50} values correlated well with the docking scores equal to −9.097 kcal/mol and −8.783 kcal/mol for hAChE and hBChE, respectively, considering that the volume of the catalytic site of BChE is much larger than that of AChE. As a result, the latter is more prone to engage in hydrophobic interactions whose contributions are more effective in enhancing docking scores.
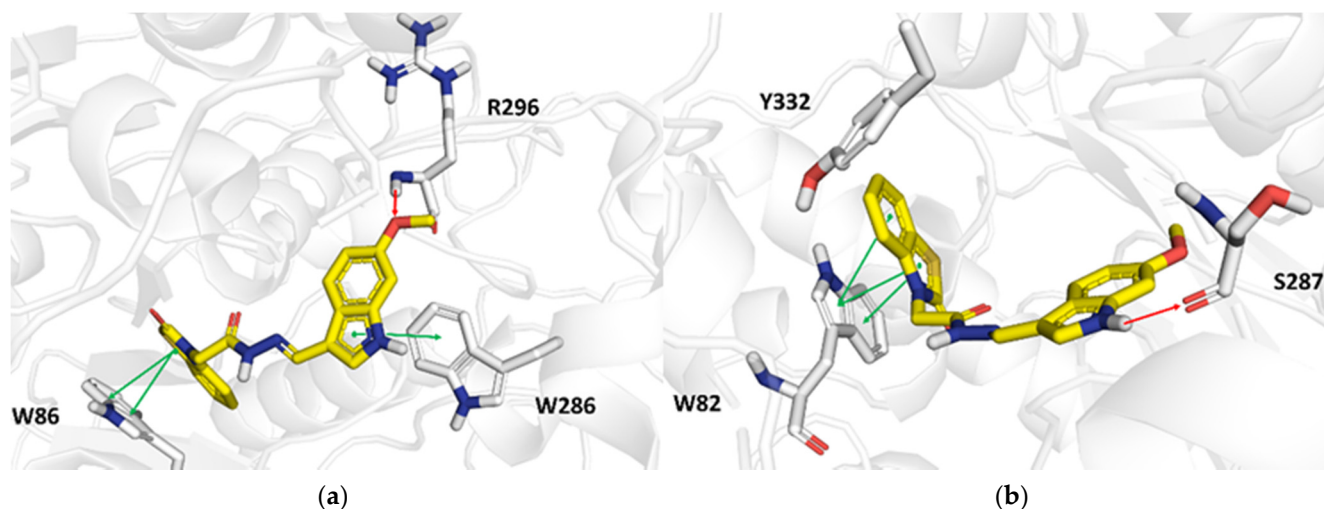
(**a**)
(**b**)

Figure 6. Docking poses carried out from docking analyses of the **M13** compound towards hAChE (PDB entry: 4EY7) (**a**) and hBChE (PDB entry: 6RUA) (**b**), respectively. Green and red arrows indicate $\pi-\pi$ interactions and hydrogen bonds, respectively. Ligands and the target residues of the binding sites are rendered in yellow and gray sticks, respectively. For the sake of completeness, all the molecular interactions observed in the docking simulations were automatically flagged by GLIDE software.

Interactions between **M13** and hAChE were observed, and the methoxy group of **M13** established a hydrogen bond with the backbone of Arg296 with a distance of 2.2 Å, whereas $\pi-\pi$ hydrophobic stacking contacts occurred between the benzothiazolone group of **M13** and the side chain of Trp286 (at a distance of 4.1 Å). The side chain of Trp86 (Figure 6a) was, instead, involved in a bidentate interaction involving the engagement of its five- and six-membered rings (at distances of 3.9 and 3.8 Å, respectively) with the benzothiazolone arm of **M13**.

As far as the interactions between **M13** and the hBChE target residues (Figure 6b) are concerned, a hydrogen bond occurred with the backbone carbonyl group of Ser287 (at a distance of 2.1 Å). Interestingly, **M13** was predicted to form hydrophobic $\pi-\pi$ interactions between the benzothiazolone group and the side chain of Trp82 (at a distance of 3.9 Å) through contacts with its five- and six-membered rings (at distances of 3.5 and 4.1 Å, respectively).

Both AChE and BChE catalyze the hydrolysis of esters and regulate the ACh concentration in glial cells, the hippocampus, and the temporal nerve cortex; therefore, ChE inhibitors can increase ACh levels to treat AD [49]. In this study, M13 was found to be a potent BChE inhibitor (IC50 = 1.21 μM) with an effective AChE inhibitory activity (IC50 = 5.03 μM).

4. Conclusions

In the study, thirteen benzothiazolone derivatives were synthesized, and their ChE and MAO inhibitory activities were investigated. The ChE inhibitory effects of the compounds were considerably higher than the MAO inhibitory effects. **M13** (IC_{50} = 1.21 $\pm$ 0.05 μM) and **M2** (IC_{50} = 1.38 $\pm$ 0.17 μM) were the most active compounds to BChE. In the kinetics and reversibility studies, the most effective compound, **M13**, was determined to be a reversible and noncompetitive inhibitor of BChE. These results suggest that **M13** is a potential BChE inhibitor to be considered a candidate agent for the treatment of Alzheimer's disease.

References

1. Brookmeyer, R.; Abdalla, N.; Kawas, C.H.; Corrada, M.M. Forecasting the prevalence of preclinical and clinical Alzheimer's disease in the United States. *Alzheimers Dement* **2018**, *14*, 121–129. [PubMed]
2. Ozdemir, Z.; Ozcelik, A.B.; Uysal, M. Approaches based on cholinergic hypothesis and cholinesterase inhibitors in the treatment of alzheimer's disease. *Front. Clin. Drug Res.-Alzheimer Disord.* **2019**, *8*, 154–190.
3. Shekari, A.; Fahnestock, M. Cholinergic neurodegeneration in Alzheimer disease mouse models. *Handb. Clin. Neurol.* **2021**, *182*, 191–209.
4. Mendiola-Precoma, J.; Berumen, L.C.; Padilla, K.; Garcia-Alcocer, G. Therapies for prevention and treatment of Alzheimer's disease. *Bio. Med. Res. Int.* **2016**, *2016*, 2589276.
5. Hampel, H.; Mesulam, M.M.; Cuello, A.C.; Farlow, M.R.; Giacobini, E.; Grossberg, G.T.; Khachaturian, A.S.; Vergallo, A.; Cavedo, E.; Snyder, P.J.; et al. The cholinergic system in the pathophysiology and treatment of Alzheimer's disease. *Brain* **2018**, *141*, 1917–1933.
6. Chen, Z.R.; Huang, J.B.; Yang, S.L.; Hong, F.F. Role of cholinergic signaling in Alzheimer's disease. *Molecules* **2022**, *27*, 1816.
7. Bekdash, R. The cholinergic system, the adrenergic system and the neuropathology of Alzheimer's disease. *Int. J. Mol. Sci.* **2021**, *22*, 1273. [CrossRef] [PubMed]
8. Bozbey, I.; Ozdemir, Z.; Uslu, H.; Ozcelik, A.B.; Senol, F.S.; Orhan, I.E.; Uysal, M. A series of new hydrazone derivatives: Synthesis, molecular docking and anticholinesterase activity studies. *Mini Rev. Med. Chem.* **2020**, *20*, 1042–1060. [PubMed]
9. Dos Santos, G.A.A.; Schmidt, C.W.P.; Forlenza, K.P. The use of esterase inhibitors. In *Pharmacological Treatment of Alzheimer's Disease*; Santos, G.A.A.D., Ed.; Springer: Cham, Switzerland, 2022. [CrossRef]
10. Gabr, M.T.; Abdel-Raziqc, M.S. Structure-based design, synthesis, and evaluation of structurally rigid donepezil analogues as dual AChE and BACE-1 inhibitors. *Bioorg. Med. Chem. Lett.* **2018**, *28*, 2910–2913. [CrossRef]
11. Dvir, H.; Silman, I.; Harel, M.; Rosenberry, T.L.; Sussmana, J.L. Acetylcholinesterase: From 3D structure to function. *Chem. Biol. Interact.* **2010**, *187*, 10–22.
12. Costanzo, P.; Cariati, L.; Desiderio, D.; Sgammato, R.; Lamberti, A.; Arcone, R.; Salerno, R.; Nardi, M.; Masullo, M.; Oliverio, M. Design, synthesis, and evaluation of donepezil-like compounds as AChE and BACE-1 inhibitors. *Med. Chem. Lett.* **2016**, *7*, 470–475. [CrossRef] [PubMed]
13. Nachon, F.; Carletti, E.; Ronco, C.; Trovaslet, M.; Nicolet, Y.; Jean, L. Crystal structures of human cholinesterases in complex with huprine W and tacrine: Elements of specificity for anti-Alzheimer's drugs targeting acetyl- and butyrylcholinesterase. *Biochem. J.* **2013**, *453*, 393–399. [CrossRef] [PubMed]
14. Leon, J.; Marco-Contelles, J. A step further towards multitarget drugs for Alzheimer and neuronal vascular diseases: Targeting the cholinergic system, amyloid-β aggregation and Ca^{2+} dyshomeostatis. *J. Curr. Med. Chem.* **2011**, *18*, 552. [CrossRef]
15. Simoni, E.; Daniele, S.; Bottegoni, G.; Pizzirani, D.; Trincavelli, M.L.; Goldoni, L.; Tarozzo, G.; Reggiani, A.; Martini, C.; Piomelli, D.; et al. Combining galantamine and memantine in multitargeted, new chemical entities potentially useful in Alzheimer's disease. *J. Med. Chem.* **2012**, *55*, 9708–9721. [CrossRef] [PubMed]
16. Nepovimova, E.; Uliassi, E.; Korabecny, J.; Peña-Altamira, L.E.; Samez, S.; Pesaresi, A.; Garcia, G.E.; Bartolini, M.; Andrisano, V.; Bergamini, C.; et al. Multitarget drug design strategy: Quinone–tacrine hybrids designedtTo block amyloid-β aggregation and to exert anticholinesterase and antioxidant effects. *J. Med. Chem.* **2014**, *57*, 8576–8589. [CrossRef]
17. Cheung, J.; Rudolph, M.J.; Burshteyn, F.; Cassidy, M.S.; Gary, E.N.; Love, J.; Franklin, M.C.; Height, J.J. Structures of human acetylcholinesterase in complex with pharmacologically important ligands. *J. Med. Chem.* **2012**, *55*, 10282–10286. [CrossRef]
18. Camps, P.; Formosa, X.; Galdeano, C.; Gomez, T.; Munoz-Torrero, D.; Scarpellini, M. Novel donepezil-based inhibitors of acetyl- and butyrylcholinesterase and acetylcholinesterase induced β-amyloid aggregation. *J. Med. Chem.* **2009**, *51*, 3588–3598. [CrossRef]
19. Bourne, Y.; Taylor, P.; Radić, Z.; Marchot, P. Structural insights into ligand interactions at the acetylcholinesterase peripheral anionic site. *EMBO J.* **2003**, *22*, 1–12. [CrossRef]
20. Tougu, V. Acetylcholinesterase: Mechanism of catalysis and inhibition. *Curr. Med. Chem. Cent. Nerv. Syst. Agents* **2001**, *1*, 155–170. [CrossRef]
21. Zhou, Y.; Wang, S.; Zhang, Y. Catalytic reaction mechanism of acetylcholinesterase determined by born-oppenheimer AB initio QM/MM molecular dynamics simulations. *J. Phys. Chem. B* **2010**, *114*, 8817–8825. [CrossRef]

22. Brus, B.; Kosak, U.; Turk, S.; Pislar, A.; Coquelle, N.; Kos, J.; Stojan, J.; Colletier, J.P.; Gobec, S. Discovery, biological evaluation, and crystal structure of a novel nanomolar selective butyrylcholinesterase inhibitor. *J. Med. Chem.* **2014**, *57*, 8167–8179. [CrossRef] [PubMed]

23. Erdogan, M.; Kilic, B.; Ilıkcı Sagkan, R.; Aksakal, F.; Ercetin, T.; Gulcan, H.O.; Dogruer, D.S. Design, synthesis and biological evaluation of new benzoxazolone/benzothiazolone derivatives as multi-target agents against Alzheimer's disease. *Eur. J. Med. Chem.* **2021**, *212*, 113124. [CrossRef] [PubMed]

24. Doğruer, D.S.; Ünlü, S.; Yeşilada, E.; Şahin, M.F. N-(2-pyridinyl)-2-[2(3H)-benzazolone-3-yl]acetamides: Synthesis, antinociceptive and anti-inflammatory activity. *Farmaco* **1997**, *52*, 745–750. [PubMed]

25. Abdelazeem, A.H.; Khan, S.I.; White, S.W.; Sufka, K.J.; McCurdy, C.R. Design, synthesis and biological evaluation of bivalent benzoxazolone and benzothiazolone ligands as potential anti-inflammatory/analgesic agents. *Bioorg. Med. Chem.* **2015**, *23*, 3248–3259. [CrossRef]

26. Jacques, P.; Pascal, C.; Evelina, C. 2(3H)-Benzoxazolone and bioisosters as "privileged scaffold" in the design of pharmacological probes. *Curr. Med. Chem.* **2005**, *12*, 877–885.

27. Akrami, H.; Mirjalili, B.H.; Khoobi, M.; Nadri, H.; Moradi, A.; Sakhteman, A.; Emami, S.; Foroumadi, A.; Shafiee, A. Indolinone-based acetylcholinesterase inhibitors: Synthesis, biological activity and molecular modeling. *Eur. J. Med. Chem.* **2014**, *84*, 375–381. [CrossRef]

28. Tripathi, P.N.; Srivastava, P.; Sharma, P.; Kumar Tripathi, M.; Seth, A.; Tripathi, A. Biphenyl-3-oxo-1,2,4-triazine linked piperazine derivatives as potential cholinesterase inhibitors with anti-oxidant property to improve the learning and memory. *Bioorg. Chem.* **2019**, *85*, 82–96. [CrossRef]

29. Raza, R.; Saeed, A.; Arif, M.; Mahmood, S.; Muddassar, M.; Raza, A.; Iqbal, J. Synthesis and Biological Evaluation of 3-Thiazolocoumarinyl Schiff-Base Derivatives as Cholinesterase Inhibitors. *Chem. Biol. Drug Des.* **2012**, *80*, 605–615. [CrossRef]

30. Özil, M.; Balaydın, H.T.; Şentürk, M. Synthesis of 5-Methyl-2,4-Dihydro-3H-1,2,4-Triazole-3-One's Aryl Schiff Base Derivatives and Investigation of Carbonic Anhydrase and Cholinesterase (AChE, BuChE) Inhibitory Properties. *Bioorganic Chem.* **2019**, *86*, 705–713. [CrossRef]

31. Ashraf, M.A.; Mahmood, K.; Wajid, A.; Maah, M.J.; Yusoff, I. Synthesis, characterization and biological activity of Schiff bases. *IPCBEE* **2011**, *10*, 185.

32. Önkol, T.; Çakir, B.; Ito, S.; Özçlik, B.; Şahin, M.F. Synthesis of some (5-chloro-2 (3H)-benzothiazolinone-3-yl) aceto/propanohydrazides towards antimicrobial and antiviral activity. *Turk. J. Pharm. Sci.* **2009**, *6*, 195–206.

33. Önkol, T.; Yildirim, E.; Erol, K.; Ito, S.; Şahin, M.F. Synthesis and antinociceptive activity of (5-chloro-2 (3H)-benzothiazolon-3-yl) propanamide derivatives. *Arch. Pharm.* **2004**, *337*, 475–481. [CrossRef] [PubMed]

34. Ellman, G.L.; Courtney, K.D.; Andres, V., Jr.; Feather-Stone, R.M. A new and rapid colorimetric determination of acetylcholinesterase activity. *Biochem. Pharmacol.* **1961**, *7*, 88–95. [CrossRef]

35. Mathew, B.; Oh, J.M.; Khames, A.; Abdelgawad, M.A.; Rangarajan, T.M.; Nath, L.R.; Agoni, C.; Soliman, M.E.S.; Mathew, G.E.; Kim, H. Replacement of chalcone-ethers with chalcone-thioethers as potent and highly selective monoamine oxidase-B inhibitors and their protein-ligand interactions. *Pharmaceuticals* **2021**, *14*, 1148. [CrossRef]

36. Alagöz, M.A.; Oh, J.M.; Zenni, Y.N.; Özdemir, Z.; Abdelgawad, M.A.; Naguib, I.A.; Ghoneim, M.M.; Gambacorta, N.; Nicolotti, O.; Kim, H.; et al. Development of a novel class of pyridazinone derivatives as selective MAO-B inhibitors. *Molecules* **2022**, *27*, 3801. [CrossRef]

37. Oh, J.M.; Jang, H.J.; Kim, W.J.; Kang, M.G.; Baek, S.C.; Lee, J.P.; Park, D.; Oh, S.R.; Kim, H. Calycosin and 8-O-methylretusin isolated from *Maackia amurensis* as potent and selective reversible inhibitors of human monoamine oxidase-B. *Int. J. Biol. Macromol.* **2020**, *151*, 441–448. [CrossRef]

38. Lee, J.P.; Kang, M.G.; Lee, J.Y.; Oh, J.M.; Baek, S.C.; Leem, H.H.; Park, D.; Cho, M.L.; Kim, H. Potent inhibition of acetylcholinesterase by sargachromanol I from *Sargassum siliquastrum* and by selected natural compounds. *Bioorg. Chem.* **2019**, *89*, 1030. [CrossRef]

39. Mathew, B.; Oh, J.M.; Abdelgawad, M.A.; Khames, A.; Ghoneim, M.M.; Kumar, S.; Nath, L.R.; Sudevan, S.T.; Parambi, D.G.T.; Agoni, C.; et al. Conjugated dienones from differently substituted cinnamaldehyde as highly potent monoamine oxidase-B inhibitors: Synthesis, biochemistry, and computational chemistry. *ACS Omega* **2022**, *7*, 8184–8197. [CrossRef]

40. Lee, H.W.; Ryu, H.W.; Kang, M.G.; Park, D.; Oh, S.R.; Kim, H. Potent selective monoamine oxidase B inhibition by maackiain, a pterocarpan from the roots of *Sophora favescens*. *Bioorg. Med. Chem. Lett.* **2016**, *26*, 4714–4719. [CrossRef]

41. Mathew, B.; Oh, J.M.; Baty, R.S.; Batiha, G.E.; Parambi, D.; Gambacorta, N.; Nicolotti, O.; Kim, H. Piperazine-substituted chalcones: A new class of MAO-B, AChE, and BACE-1 inhibitors for the treatment of neurological disorders. *Environ. Sci. Pollut. Res. Int.* **2021**, *28*, 38855–38866. [CrossRef]

42. Pajk, S.; Knez, D.; Košak, U.; Zorović, M.; Brazzolotto, X.; Coquelle, N.; Nachon, F.; Colletier, J.P.; Živin, M.; Stojan, J.; et al. Development of potent reversible selective inhibitors of butyrylcholinesterase as fluorescent probes. *J. Enzym. Inhib. Med. Chem.* **2020**, *35*, 498–505. [CrossRef] [PubMed]

43. *Schrödinger Release 2021-4: Protein Preparation Wizard*; Epik, Schrödinger, LLC: New York, NY, USA; Impact, Schrödinger, LLC: New York, NY, USA; Prime, Schrödinger, LLC: New York, NY, USA, 2021.

44. *Schrödinger Release 2021-4: LigPrep*; Schrödinger, LLC: New York, NY, USA, 2021.

45. *Schrödinger Release 2021-4: Glide*; Schrödinger, LLC: New York, NY, USA, 2021.

46. Friesner, R.A.; Banks, J.L.; Murphy, R.B.; Halgren, T.A.; Klicic, J.J.; Mainz, D.T.; Repasky, M.P.; Knoll, E.H.; Shelley, M.; Perry, J.K.; et al. Glide: A new approach for rapid, accurate docking and scoring. 1. Method and assessment of docking accuracy. *J. Med. Chem.* **2004**, *47*, 1739–1749. [CrossRef] [PubMed]
47. Jeong, G.S.; Kang, M.G.; Lee, J.Y.; Lee, S.R.; Park, D.; Cho, M.; Kim, H. Inhibition of butyrylcholinesterase and human monoamine oxidase-B by the coumarin glycyrol and liquiritigenin isolated from *Glycyrrhiza uralensis*. *Molecules* **2020**, *25*, 3896. [CrossRef] [PubMed]
48. Heo, J.H.; Eom, B.H.; Ryu, H.W.; Kang, M.G.; Park, J.E.; Kim, D.Y.; Kim, J.H.; Park, D.; Oh, S.R.; Kim, H. Acetylcholinesterase and butyrylcholinesterase inhibitory activities of khellactone coumarin derivatives isolated from *Peucedanum japonicum* Thurnberg. *Sci. Rep.* **2020**, *10*, 21695. [CrossRef]
49. Oh, J.M.; Kang, Y.; Hwang, J.H.; Park, J.H.; Shin, W.H.; Mun, S.K.; Lee, J.U.; Yee, S.T.; Kim, H. Synthesis of 4-substituted benzyl-2-triazole-linked-tryptamine-paeonol derivatives and evaluation of their selective inhibitions against butyrylcholinesterase and monoamine oxidase-B. *Int. J. Biol. Macromol.* **2022**, *217*, 910–921. [CrossRef]